

## Experimental Communication

### Cite

Ganguly U, Bir A, Chakrabarti S (2022) Cytotoxicity of mitochondrial Complex I inhibitor rotenone: a complex interplay of cell death pathways. MitoFit Preprints 2022.13.v2. <https://doi.org/10.26124/mitofit:2022-0013.v2>

### Author contributions

Data collection and evaluation was performed by UG, AB, SC. All authors wrote the manuscript.

### Conflicts of interest

The authors declare they have no conflict of interest.

Received 2022-08-08

Accepted 2022-08-16

Online 2022-11-10




### Data availability

Data are not available in open repository but may be obtained from the corresponding author.

### Keywords

rotenone;  
 mitochondria;  
 ferroptosis;  
 reactive oxygen species;  
 neurodegeneration

# Cytotoxicity of mitochondrial Complex I inhibitor rotenone: a complex interplay of cell death pathways

 Upasana Ganguly<sup>1</sup>,  Aritri Bir<sup>2</sup>,  
 Sasanka Chakrabarti<sup>1\*</sup>

<sup>1</sup> Department of Biochemistry and Central Research Laboratory, Maharishi Markandeshwar Institute of Medical Sciences and Research, Maharishi Markandeshwar University (Deemed to be), Mullana, Ambala, India

<sup>2</sup> Department of Biochemistry, Dr. B.C. Roy Multispeciality Medical Research Centre, IIT Kharagpur, India

\* Corresponding author: [profschakrabarti95@gmail.com](mailto:profschakrabarti95@gmail.com)

## Summary

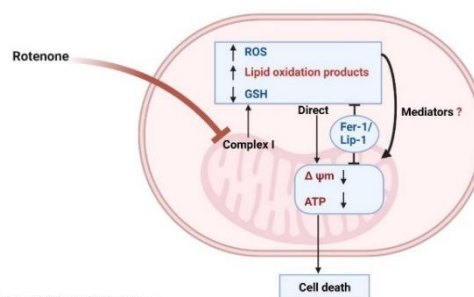


Image created using BioRender.com

Ferroptosis has been identified as a type of regulated cell death triggered by a diverse set of agents with implications in various diseases

like cancer and neurodegenerative diseases like Parkinson's disease. Because the classical mitochondrial Complex I inhibitor rotenone is widely used to develop the experimental models of Parkinson's disease, we have examined if rotenone is an inducer for ferroptosis. Ferroptosis is iron-dependent and accompanied by an accumulation of reactive oxygen species (ROS) and lipid oxidation products, a depletion of reduced glutathione, mitochondrial morphological alterations, and the rupture of cell membrane; the process is inhibited by specific antioxidants like ferrostatin-1 and liproxstatin-1 and by other general antioxidants like the iron-chelator deferoxamine, vitamin E and N-acetylcysteine. However, the mechanism of cell death in ferroptosis subsequent to the accumulation of ROS and lipid oxidation products is not clearly established. We show here that rotenone (0.5  $\mu$ M) causes the death of SH-SY5Y cells (a human neuroblastoma cell line) for 48 h

accompanied by mitochondrial membrane depolarization and intracellular ATP depletion. This is associated with an intracellular accumulation of ROS and the lipid oxidation product malondialdehyde or MDA and a decrease in reduced glutathione content. All these processes are inhibited very conspicuously by specific inhibitors of ferroptosis such as ferrostatin-1 and liproxstatin-1. However, the decrease in Complex I activity upon rotenone-treatment of SH-SY5Y cells is not significantly recovered by ferrostatin-1 and liproxstatin-1. When the rotenone-treated cells are analyzed morphologically by Hoechst 33258 and propidium iodide (PI) staining, a mixed picture is noticed with densely fluorescent and condensed nuclei indicating apoptotic death of cells (Hoechst 33258) and also significant numbers of necrotic cells with bright red nuclei (PI staining).

In brief, we have shown that in SH-SY5Y cells rotenone is an inducer of ferroptosis, and the cells present mixed morphological features of apoptosis and necrosis.

## 1. Introduction

An important sub-type of regulated cell death (RCD) called ferroptosis has been under intensive investigation over the last few years, and the process has been implicated in different diseases, including cancer and neurodegenerative diseases (Li et al 2020; Jiang et al 2021). Ferroptosis is an iron-dependent pathway of RCD which is accompanied by an excess production of reactive oxygen species or ROS, lipid-derived oxyradicals, and various lipid peroxidation products; in a broad sense the term ROS includes not only the classical reactive oxygen species like the superoxide radical, H<sub>2</sub>O<sub>2</sub> and hydroxyl radicals, but also the lipid hydroperoxides, lipid and protein derived oxyradicals, peroxy nitrite radicals and many others (Stockwell et al 2017; Cheng et al 2018). Along with the accumulation of ROS, a depletion of glutathione, mitochondrial morphological alterations, and the rupture of the cell membrane occur; the process is inhibited by iron-chelator like deferoxamine and lipophilic antioxidants such as vitamin E, butylated hydroxytoluene, ferrostatin-1 (Fer-1) and liproxstatin-1 (Lip-1) (Xie et al 2016; Stockwell et al 2017). The ferroptotic death of cells apparently requires an accumulation of lipid peroxidation intermediates and products, and thus novel lipophilic antioxidants like Fer-1 and Lip-1 are particularly good in preventing ferroptosis (Zilka et al 2017). Ferroptosis can be triggered by many different pharmacological agents, which cause a depletion or decreased synthesis of the major intracellular antioxidant like reduced glutathione (GSH) or inhibit the antioxidant enzyme glutathione peroxidase 4 (Gpx4), or cause an increase in the intracellular iron content (Jiang et al 2021; Li et al 2020). Several pathways regulating or initiating ferroptosis in cells have been identified primarily by genetic studies, but definite mechanisms or mediators executing cell death following the accumulation of ROS and lipid oxidation products are yet to be established in ferroptosis. Mitochondria being the most important source of ROS generation *in vivo*, it is also important to investigate how mitochondrial bioenergetic alterations are involved in ferroptotic death of cells. In fact, mitochondrial respiratory chain inhibitors and TCA cycle

intermediates have been implicated in complex and contradictory ways with ferroptosis (Gao et al 2019; Yao et al 2021; Gan 2021).

Linking the process of ferroptosis with neuronal death in neurodegenerative diseases like Alzheimer's disease (AD) or Parkinson's disease (PD) appears to be an attractive proposition because both increased iron accumulation and oxidative damage in specific brain regions are key pathological features of these diseases (Ganguly et al 2017). Unlike AD, several toxins-based animal models are quite popular in analyzing PD pathogenesis or screening for potential anti-parkinsonian drugs (Duty, Jenner 2011; Betarbet et al 2002). Despite the limitations of cell-based models to recreate the pathologic scenario of a complex disease like PD, the cytotoxic mechanisms of several PD-related toxins like 1-methyl-4-phenyl-1,2,3,6-tetrahydropyridine (MPTP), 6-hydroxydopamine, rotenone have been extensively studied in different cell lines and primary cultures of neurons (Ke et al 2021). Rotenone, the classical inhibitor of mitochondrial Complex I, causes cell death, redox imbalance, and impaired mitochondrial bioenergetics in different experimental models, but the mechanisms of cytotoxicity of rotenone are not fully elucidated and the nature of cell death as reported in published reports is quite varied (Barrientos, Moraes 1999; Moon et al 2005; Radad et al 2006; Xiong et al 2013; Callizot et al 2019). For example, from an elaborate study where Complex I inhibition was induced by genetic manipulation or by rotenone treatment, it was concluded that rotenone-induced cell death could be ascribed to increased oxidative stress instead of a simple ATP depletion as a result of Complex I inhibition (Barrientos, Moraes 1999). Likewise, rotenone-induced death in SK-N-MC (human neuroblastoma cell line) cells was prevented by  $\alpha$ -tocopherol, and increased oxidative stress as a result of Complex I inhibition was suggested to be the mechanism of neural cell death under this condition (Sherer et al 2003). On the other hand, another study distinguished two different mechanisms of rotenone-induced death in dopaminergic and non-dopaminergic neuronal cells. Thus, in non-dopaminergic MN9X cells, rotenone caused oxidative damage mediated death, while rotenone-mediated death of dopaminergic MN9D cells was attributed to the mitochondrial bioenergetic disruption from Complex I inhibition (Kweon et al 2004). Similarly, rotenone at low concentrations caused the death of primary ventral mesencephalic neurons of rats by Complex I inhibition and associated mitochondrial membrane depolarization, and the process was not prevented by several antioxidants (Moon et al 2005). Thus, the exact pathway of rotenone-induced cell death is still somewhat unclear, and it may partly depend upon the dose of rotenone and the nature of the cell line used. Furthermore, the nature of cell death induced by rotenone is again debatable to some extent, and apoptosis, autophagy, and necrosis have all been suggested in different studies (Barrientos, Moraes 1999; Callizot et al 2019; Xiong et al 2013; Radad et al 2006). Some interesting links between rotenone cytotoxicity, ferroptosis and intracellular iron dyshomeostasis have been indicated also in some studies. Thus, the rotenone-induced ROS production, typical morphological changes,  $\alpha$ -synuclein aggregation, and activation of apoptosis in SH-SY5Y cells could be prevented by ferrostatin-1 which is a typical antioxidant trapping lipid-derived oxyradicals and inhibiting ferroptosis (Kabiraj et al 2015). Likewise, another interesting study reported that the rotenone exposure of SH-SY5Y cells increased the levels of transferrin receptor 1 and divalent metal transporter 1 but decreased the cellular level of ferroportin 1; these changes led to an increase in the iron uptake with an increase in the intracellular labile pool of iron and consequent oxidative stress (Urrutia et al 2017). This study further showed that the knockdown of iron-responsive element binding protein 1 (IRP-1)

prevented rotenone-induced iron dyshomeostasis, oxidative stress, and cell death (Urrutia et al 2017).

Over this backdrop and given the fact that mitochondrial dysfunction and ferroptotic death are possibly interlinked in the pathogenesis of Parkinson's disease, we were prompted to re-examine the rotenone-induced death of SH-SY5Y cells with a focus on ferroptosis and mitochondria. SH-SY5Y cells were selected for this study because this catecholaminergic human neuroblastoma cell line is widely used to investigate the mechanisms of PD neurodegeneration (Xicoy et al 2017).

## 2. Materials and methods

### 2.1. Cell culture and treatment protocol

SH-SY5Y cells undifferentiated (purchased from NCCS, Pune, India) were maintained in a medium composed of 2 volumes of Dulbecco's modified Eagle's medium (DMEM, ThermoFisher, USA) and 1 volume of Ham's F12 medium containing 10% fetal bovine serum (ThermoFisher, USA); penicillin 50 units/mL, streptomycin 50 µg/mL (Penicillin-Streptomycin, ThermoFisher, USA), and amphotericin B (Sigma, USA) 2.5 µg/mL were also present in the medium. The medium also contained glucose and glutamine. For experimental purposes, the cells were grown and manipulated in plastic tissue culture flasks or multi-well tissue culture plates, or poly-L-lysine coated coverslips under a humidified atmosphere of 5% CO<sub>2</sub> and 95% air at 37<sup>o</sup> C. The cells were treated without (control) or with rotenone (Sigma, USA) (0.5 µM) for 48 h in the presence or absence of ferrostatin-1 or Fer-1 (Sigma, USA) (1 µM, Sigma, USA), liproxstatin-1 or Lip-1 (Sigma, USA) (1 µM), or other additions followed by the analysis of various biochemical and microscopic parameters.

### 2.2. Measurement of cell viability

The cell viability was assessed by Trypan blue assay as well as by LDH release assay (Ganguly et al 2020). In Trypan blue assay, the dead (blue-stained) and live cells were counted by an automated cell counter (ThermoFisher Scientific, USA), which was cross-verified by manual counting by two observers each counting 250 – 300 cells. In addition, the LDH released in the medium in each well was assayed spectrophotometrically by monitoring the oxidation of NADH (SRL, India) at 340 nm using pyruvate as the substrate; the activity of the enzyme released in each well was normalized with the protein content and then expressed as a percentage of LDH released in reference wells with 100% cell death (cells treated with 10 µM antimycin A purchased from Sigma, USA) (Ganguly et al 2020).

### 2.3. Measurements of oxidative stress parameters

ROS production and the cellular levels of malondialdehyde (MDA) and reduced glutathione were measured as oxidative stress parameters in control and various groups of treated SH-SY5Y cells. For ROS measurement, the fluorogenic ROS probe, 2', 7'-dichlorodihydrofluorescein diacetate or H<sub>2</sub>DCFDA (Sigma, USA), was utilized; intracellular esterases hydrolyzed H<sub>2</sub>DCFDA to release DCFH<sub>2</sub>, which reacted with ROS to produce a fluorescent product (λ<sub>ex</sub> 485 nm, λ<sub>em</sub> 535 nm) (Jana et al 2011). The assay was conducted with the cells in 96-well plates; after removal of the medium, each well was

gently rinsed twice with phosphate-buffered saline, pH 7.4 (PBS), removing dead cells and debris. The adherent cells were incubated with a serum-free medium containing 10  $\mu$ M H<sub>2</sub>DCFDA at 37<sup>o</sup> C for 30 min in the dark, followed by removal of the medium and two washings with the PBS. The cells in each well were finally covered with 200  $\mu$ l of PBS, and the fluorescence intensity was measured in a multi-mode plate reader (Molecular Devices, USA). It may be mentioned here that H<sub>2</sub>DCFDA is not a specific probe for any particular member of ROS, but interacts with H<sub>2</sub>O<sub>2</sub>, hydroxyl radicals, lipid hydroperoxides, peroxynitrite, and peroxy radicals; in a broad sense as indicated already, ROS encompasses all these radicals, and several others (Gomes et al 2005; Kalyanaraman et al 2012; Cheng et al 2018). However, the reaction chemistry of H<sub>2</sub>DCFDA assay is complex and it can be affected by several intracellular components like cytochrome c, heme, and transition metals (Dikalov, Harrison 2014).

The cellular content of GSH was determined by 5,5'-dithio-bis-nitrobenzene or DTNB (Sigma, USA) assay. After brief washings in PBS, the cells were re-suspended in 100 mM potassium phosphate buffer / 5 mM EDTA, pH 7.5 (KPE buffer), extracted by brief vortexing with an equal volume of 0.1% Triton X-100 in 5% trichloroacetic acid in KPE buffer and centrifuged at 4<sup>o</sup> C at 10,000 rpm for 5 min. The supernatant was used to measure GSH by allowing it to react with DTNB in KPE buffer at 37<sup>o</sup> C for 10 min, and the color developed was read at 412 nm. The method was adapted from the published procedures (Rahman et al 2006; Look et al 1997).

The measurement of MDA was based on 2-thiobarbituric acid or TBA (HiMedia, India) assay as obtained from published procedures (Draper et al 1993).

#### **2.4. Measurement of mitochondrial parameters**

The mitochondrial membrane potential and ATP content of control and treated SH-SY5Y cells were measured by tetramethylrhodamine ethyl ester or TMRE (Sigma, USA) and luciferin-luciferase-based assays respectively as published earlier by our group (Ganguly et al 2020; Singh et al 2022). Briefly, the control and treated cells were maintained on 96 well plates for 48 h, and after the incubation, the medium from each well was removed followed by two gentle washings with 200  $\mu$ L of phosphate-buffered saline (PBS) to remove the dead cells and the debris, and the adherent cells were analyzed for mitochondrial membrane potential or cellular ATP content.

In the case of TMRE assay, the adherent cells were further incubated in serum-free medium with 100 nM of TMRE for 15 min at 37<sup>o</sup> C. At the end of the incubation, the medium was removed and the attached cells were delicately washed with PBS twice and then covered with 100  $\mu$ L of PBS. Finally, the fluorescence intensity was recorded at  $\lambda_{ex}$  549 nm and  $\lambda_{em}$  575 nm in a multi-mode plate reader (Molecular Devices, USA). The values were expressed as percentages of the control after normalization with the protein content of the corresponding wells. With each experimental set of TMRE assay, carbonyl cyanide 4-(trifluoromethoxy) phenylhydrazone or FCCP [Sigma, USA]-treated cells were analyzed as positive controls for membrane depolarization.

For ATP assay, the adherent cells (control and treated) were lysed with an ice-cold hypotonic buffer containing 10 mM Tris, 1 mM EDTA, 0.5% Triton X-100, pH 7.6. The cell lysate was mixed immediately with the ATP assay mix as per the manufacturer's protocol (Sigma, USA) and the chemiluminescence readings from different wells were recorded using a multi-mode microplate reader (Molecular Devices, USA). A calibration curve of ATP (0.08 – 40 nM) was used to calculate the actual concentration of ATP in the cell lysate.

For the assay of Complex I-III (NADH-cytochrome c reductase activity), mitochondria were isolated from the cells as described earlier (Jana et al 2011). Complex I-III assay was performed spectrophotometrically using NADH as the electron donor and ferricytochrome c (Sigma, USA) as the electron acceptor. The reaction was monitored by following the rate of reduction of ferricytochrome c at 540 nm (Bagh et al 2011).

## 2.5. Nuclear staining by Hoechst and propidium iodide (PI)

Hoechst 33258 dye (Invitrogen, USA) was used for the identification of apoptotic nuclei (Jana et al 2011). SH-SY5Y cells were grown on poly-L-lysine coated coverslips and treated without (control) or with rotenone (0.5  $\mu$ M) for 48 h. The cells were washed twice with PBS, fixed with 4% paraformaldehyde for 10 min, and re-washed twice with PBS. The fixed cells were then incubated with 1  $\mu$ g/ml Hoechst 33258 dye for 20 min at 37<sup>o</sup> C. After staining, the coverslips were rinsed with PBS, mounted on glass slides, and observed under a fluorescence microscope (Carl Zeiss, Germany). For PI staining, control and treated cells grown on 24-well plates were trypsinized into suspensions, centrifuged and the pelleted cells fixed with 70% ethanol for 10 min. The cells were then washed twice with PBS and re-suspended in PBS with PI (ThermoFisher, USA) (1  $\mu$ M) for 20 min at 37<sup>o</sup> C. The stained cells were collected by centrifugation, washed with PBS twice to remove the excess dye, and observed under a fluorescence microscope (Carl Zeiss, Germany).

## 2.6. Protein quantification

Protein quantification was performed by bicinchoninic acid or BCA (Sigma, USA) assay (Smith et al 1985). The samples were solubilized in 1% sodium dodecyl sulfate (SDS) before the estimation of protein.

## 2.7. Statistical analysis

Statistical significance among three or more groups was performed by one-way analysis of variance (ANOVA) followed by Tukey's posthoc test after checking for the normality of data distribution. A p-value of  $\leq 0.05$  was considered statistically significant. Values are represented as the medians with range and scatterplots reflecting the individual data points. GraphPad Prism version 8.4.2 was used for the statistical calculations.

## 3. Results

Results presented in Fig.1 show that rotenone (0.5  $\mu$ M) caused a marked loss of cell viability after 48 h of incubation; a comparable and more than a 5.5-fold increase of cell death with respect to control cells could be seen both in Trypan blue and LDH release assays. The cell death was prevented to a large extent when the cells were co-incubated with Fer-1 (1  $\mu$ M) or Lip-1 (1  $\mu$ M) along with rotenone (Figure 1).

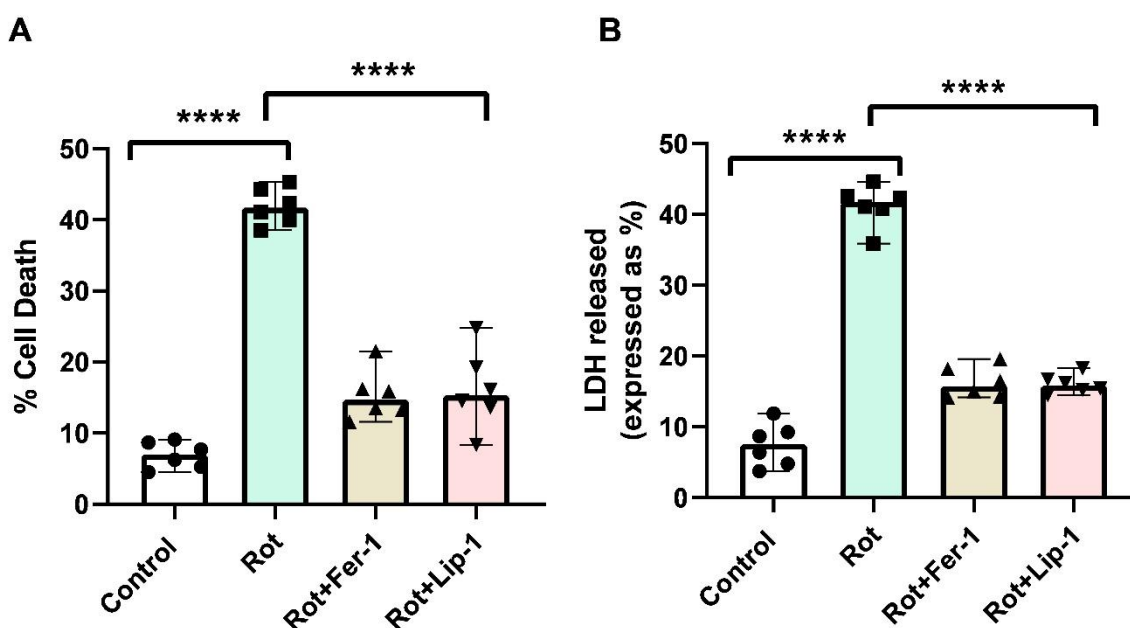


**Figure 1. Ferrostatin-1 and Liproxstatin-1 prevent rotenone-induced cell death.** SH-SY5Y cells were treated without (Control) or with Rotenone (Rot, 0.5  $\mu$ M) in the presence or absence of ferrostatin-1 (Fer-1, 1  $\mu$ M) or liproxstatin-1 (Lip-1, 1  $\mu$ M) for 48 h. The cell viability was analyzed by (A) Trypan blue assay and (B) LDH release assay as described in the Materials and Methods. Values are medians with range of six observations (independent) shown as scatterplots of individual data points. Statistically significant, \*\*\*\* $p < 0.0001$ .

When SH-SY5Y cells were incubated with rotenone (0.5  $\mu$ M) for 48 h, a nearly 4.5-fold increase in the level of MDA, an end product of lipid peroxidation, could be seen compared to that in control cells which was abolished nearly completely by co-treatment with Fer-1 and Lip-1. The generation of ROS on rotenone-treated SH-SY5Y cells increased strikingly over the control value (by about 4.5 folds) which could be prevented markedly by Fer-1 or Lip-1 (Figure 2). The major cellular antioxidant GSH was depleted noticeably on rotenone-treatment of SH-SY5Y cells for 48 h which could be mostly rescued by the co-treatment with Fer-1 and Lip-1 (Figure 2).

Three important parameters related to mitochondrial functions were affected by the rotenone-treatment of SH-SY5Y cells for 48 h as presented in Fig.3. Mitochondrial transmembrane potential and cellular ATP content were decreased by nearly 60% when SH-SY5Y cells were incubated for 48 h with 0.5  $\mu$ M rotenone, and both these phenomena were markedly, but not completely, prevented by the co-treatment of the cells with Fer-1 and Lip-1 (Figure 3). Complex I-III (NADH-cytochrome c reductase) activity was inhibited by about 50% after the rotenone-treatment of SH-SY5Y cells for 48 h, but Fer-1 or Lip-1 did not show any statistically significant protection against rotenone (Figure 3).

When SH-SY5Y cells were treated with rotenone (0.5  $\mu$ M) for 48 h and the cells were examined under a fluorescence microscope after staining with Hoechst 33258, many brightly fluorescent and condensed nuclei could be noticed indicating apoptotic cells; likewise, an examination of PI-stained cells after similar rotenone-treatment revealed many bright red fluorescent nuclei indicative of cell membrane rupture and necrosis (Figure 4).

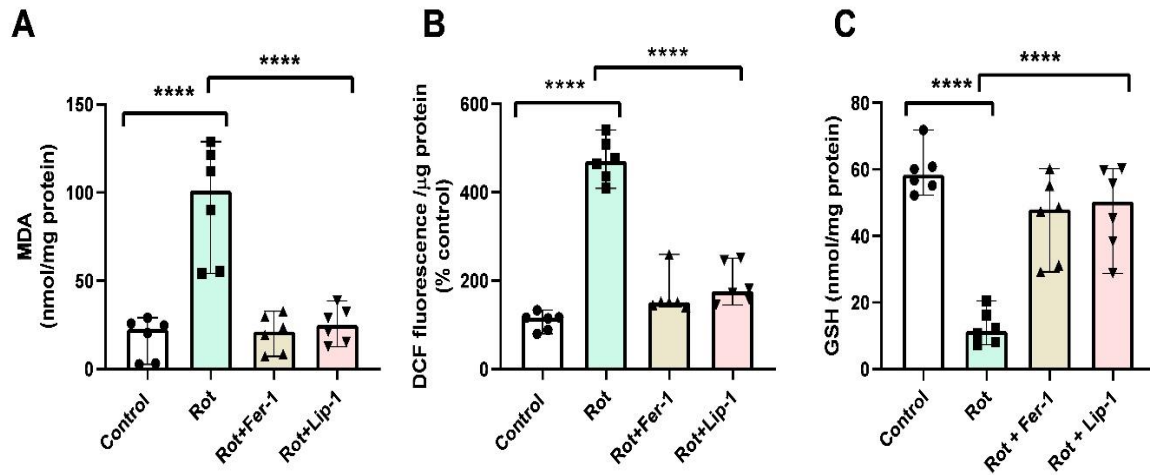


**Figure 2. Rotenone-mediated oxidative stress in SH-SY5Y cells.** SH-SY5Y cells were treated without (Control) or with Rotenone (Rot, 0.5 μM) in the presence or absence of ferrostatin-1 (Fer-1, 1 μM) or lipoxstatin-1 (Lip-1, 1 μM). After 48h of incubation, the cells were analyzed for MDA (A), ROS (B), and GSH (C) content as described in the Materials and Methods. Values are represented as medians with range of six independent experiments. \*\*\*\* $p < 0.0001$  denotes the level of significance.

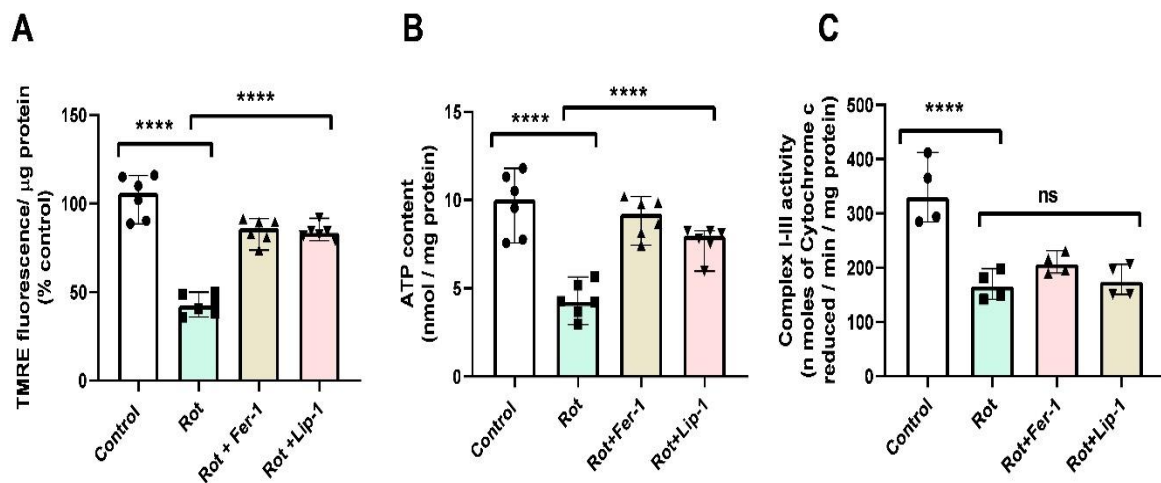


**Figure 3. Effects of Ferrostatin-1 and Lipoxstatin-1 on rotenone-mediated mitochondrial dysfunction.** SH-SY5Y cells were either untreated (Control) or treated with rotenone (Rot, 0.5 μM) with or without ferrostatin-1 (Fer-1, 1 μM) or lipoxstatin-1 (Lip-1, 1 μM) for 48 h. The cells were analyzed for (A) mitochondrial membrane potential using TMRE assay, (B) intracellular ATP content, or (C) mitochondrial Complex I-III activity. The experiments were performed in six biological replicates for (A) and (B) and four biological replicates for (C). Values are represented as medians with range indicating individual data points in scatterplots. Statistically significant, \*\*\*\* $p < 0.0001$ . ns, non-significant.



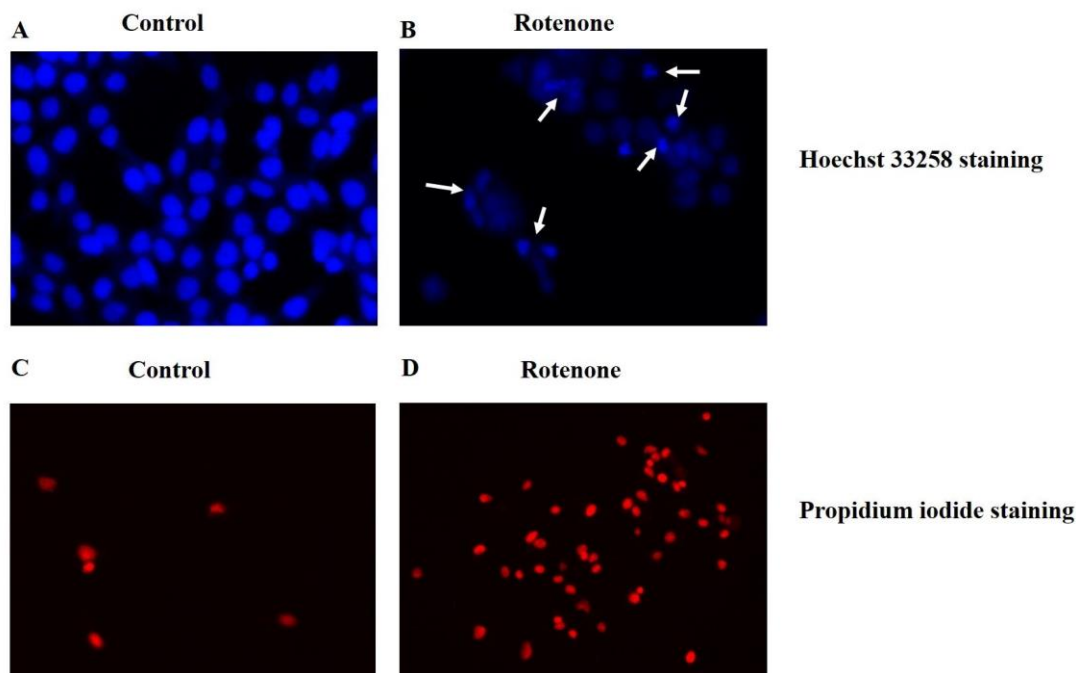


**Figure 4. Nuclear staining Hoechst 33258 and PI.** SH-SY5Y cells were treated without (Control) or with Rotenone (0.5  $\mu$ M) for 48 h. The cells were stained by Hoechst 33258 (**A & B**) or PI (**C & D**) as described in the Materials and Methods. A representative image from a set of 4 independent experiments. The white arrows indicate the apoptotic nuclei (**B**).

## 4. Discussion

The inhibition of mitochondrial Complex I (measured as NADH-ubiquinone reductase) as well as NADH-cytochrome c reductase was initially observed in the substantia nigra of postmortem PD brains, and subsequently, other mitochondrial anomalies were also reported in this disease from similar postmortem studies (Schapira et al 1990; Toulorge et al 2016). At the experimental level, complex I inhibitors like MPTP and rotenone are popular toxins to develop animal models of PD (Duty, Jenner 2011; Richardson et al 2007). However, the mechanisms of rotenone cytotoxicity are not, definitely established, as already indicated at the beginning of this article. Though several studies suggested that a simple bioenergetic failure of the cell from mitochondrial complex I inhibition by rotenone could trigger cell death, other studies demonstrated the predominant role of oxidative stress in this process (Barrientos, Moraes 1999; Sherer et al 2003; Li et al 2003; Kweon et al 2004; Moon et al 2005). In an elegant study with dopaminergic neurons obtained from *Ndufs4* (a gene necessary for complex I assembly)-deficient mice, it was shown that rotenone toxicity was not prevented in cells deficient in Complex I activity implying other mechanisms and targets of rotenone toxicity (Choi et al 2008). It is quite possible that increased production of ROS with associated oxidative stress could be the pivotal mechanism of cytotoxicity in rotenone-treated cells given the known involvement of ROS in differently regulated cell death pathways. The enhanced formation of ROS could be the result of Complex I inhibition by rotenone, but other mechanisms may also be involved such as the increased intracellular labile pool of iron as

a result of altered expression levels of different iron-transport proteins in rotenone-treated cells (Urrutia et al 2017).

Our current study demonstrated that rotenone could induce cell death and an increased accumulation of ROS and lipid peroxidation end products, and depletion of GSH, which were all prevented markedly by typical inhibitors of ferroptosis like Fer-1 and Lip-1; thus, these observations are indicative of rotenone-induced ferroptosis under our experimental conditions. Although mitochondrial morphological changes have been characteristically described in ferroptosis, the precise involvement of mitochondria in ferroptosis has remained controversial in many respects (Gao et al 2019; Gan 2021; Wang et al 2020). For example, mitochondrial membrane hyperpolarization was reported by classical inducers of ferroptosis such as erastin (Gao et al 2019). On the other hand, t-butyl hydroperoxide was shown to trigger ferroptosis in PC12 cells with mitochondrial membrane depolarization and loss of ATP, and our results are consistent with this study (Wu et al 2018). In melanoma cells also, the mitochondrial complex I inhibitor BAY 87-2243 was reported to cause ferroptosis and necroptosis with mitochondrial membrane depolarization (Basit et al 2017). Our results further show that Fer-1 and Lip-1 rescued the rotenone-induced loss of mitochondrial membrane potential and cellular ATP content, but not inhibition implying that the latter phenomenon *per se* was not responsible for mitochondrial bioenergetic impairment. Instead, the accumulation of ROS and lipid peroxidation products in rotenone-treated cells was responsible for mitochondrial dysfunction and cell death. Our results are, therefore, in conformity with those studies that suggested oxidative stress instead of a bioenergetic failure from direct Complex I inhibition as the key mechanism of rotenone toxicity (Barrientos, Moraes 1999; Sherer et al 2003; Li et al 2003). This oxidative stress-mediated cell death upon rotenone exposure gains further support from an interesting study that showed activation of oxidative stress-sensitive kinases like p38 and c-Jun N-terminal protein kinase (JNK) in SH-SY5Y cells after rotenone treatment which was linked with the apoptotic cell death (Newhouse et al 2004). In a recently published study related to the rotenone toxicity in SH-SY5Y cells, we reported that mitochondrial membrane depolarization, decreased cellular ATP content, increased ROS production, and cell death at 48 h of rotenone exposure were markedly prevented by cyclosporine A implying that these effects were the result of activation of mitochondrial permeability transition pore or mPTP (Singh et al 2022). In the same study, we further showed that the cell death and ROS production in rotenone-treated cells during the early phase of exposure at 4 h or 24 h was much less compared to that at 48 h and was not noticeably preventable by cyclosporine A (Singh et al 2022). These results tend to suggest that during rotenone exposure an initial increase of ROS production occurs presumably by Complex I inhibition resulting in some cell death, but gradually the build-up of ROS through free radical chain reactions activates the mPTP leading to pronounced cell death, mitochondrial impairment and further ROS production at the later phase. This scenario agrees well with the results of the current study; Fer-1 and Lip-1 prevented the build-up of ROS and the oxidative stress during rotenone exposure and thereby blocked the subsequent mPTP activation. Thus, Fer-1 and Lip-1 prevented mitochondrial impairment, cell death, and further ROS production observed at 48 h in the current study. It is not known at this juncture if ROS directly activates mPTP, or other mediators are involved in this process. Interestingly in the current study, the Hoechst 33258 and PI staining of SH-SY5Y cells after rotenone treatment for 48 h indicated a mixed pattern of necrosis and apoptosis which was expected given the involvement of mPTP in this process. The activation of mPTP is mechanistically linked with both

apoptosis and necrosis (Kinnally et al 2011; Redza-Dutordoir et al 2016). This mixed pattern of apoptosis and necrosis in rotenone-treated cells was also reported earlier by others (Radad et al 2006; Hong et al 2014).

Though our study has demonstrated the central role of ROS and oxidative stress in rotenone cytotoxicity, it does not explain why in some other studies the direct bioenergetic failure as from Complex I inhibition by rotenone was shown to be the underlying mechanism of cell death (Moon et al 2005; Kweon et al 2004). It is possible that during the early phase or under lower doses of rotenone exposure or with certain types of cells the alternative mechanism (Complex I induced bioenergetic failure) is operative. It is necessary to delineate these two different mechanisms of cell death by carefully controlling the two mechanisms under different experimental conditions. Likewise, the nature of the cells (primary neurons dopaminergic or non-dopaminergic, differentiated or undifferentiated neural cell lines or non-neural cell lines) will have a significant influence on the mechanism of rotenone toxicity which should be explored thoroughly. It would be interesting also to examine the effects of ferroptosis inhibitors like Fer-1 and Lip-1 on rotenone toxicity under different experimental conditions. However, in the current study where the oxidative mechanism of rotenone toxicity is operative, it is understandable why molecules like Fer-1, Lip-1, and cyclosporine A are capable of preventing cell death without recovering the Complex I activity (Singh et al 2022). It is tempting to speculate that under conditions of the oxidative mechanism of rotenone toxicity some metabolic re-programming compensates for the bioenergetic impairment of Complex I inhibition but cannot rescue the cells from oxidative death. Thus, it would be interesting to explore this aspect of metabolic re-programming in rotenone-treated cells under two different mechanisms of cell death *vis-à-vis* the protective role of Fer-1, Lip-1, or cyclosporine A. Additionally, it may be mentioned that some studies also indicated other toxic effects of rotenone at higher concentrations like the disorganization of microtubular structures that were linked with the process of apoptosis (Barrientos, Moraes 1999).

In conclusion, our short report implicates rotenone as a ferroptotic inducer, and further implies the involvement of mitochondria in ferroptotic death. When analyzed in combination with another related recent publication of our group, it is evident that the mPTP activation is a key event of ferroptotic death which exhibits the features of both apoptosis and necrosis. Further, we have suggested from a survey of the existing studies and our results how rotenone toxicity could follow different mechanisms under different experimental conditions. At the translational level, the results are important also because ferroptosis is now considered a possible mechanism of neurodegeneration in PD, and rotenone is widely used to develop experimental models of PD. The neuroprotective potential of Fer-1 or Lip-1 in animal models of PD should be explored further for a new therapeutic approach for PD.

## Abbreviations

AD	Alzheimer's disease	mtPTP	mitochondrial permeability transition pore
GSH	reduced glutathione	PD	Parkinson's disease
MDA	malondialdehyde	ROS	reactive oxygen species
MPTP	1-methyl-4-phenyl-1,2,3,6-tetrahydropyridine		

## Acknowledgements

S.C. acknowledges the financial support received from Indian Council of Medical Research (ICMR), Government of India [Sanction No. 5/4-5/191/Neuro/2019-NCD-I].

## References

- Bagh MB, Thakurta IG, Biswas M, Behera P, Chakrabarti S (2011) Age-related oxidative decline of mitochondrial functions in rat brain is prevented by long term oral antioxidant supplementation. <https://doi.org/10.1007/s10522-010-9301-8>
- Barrientos A, Moraes CT (1999) Titrating the effects of mitochondrial ccomplex I impairment in the cell physiology. <https://doi.org/10.1074/jbc.274.23.16188>
- Basit F, van Oppen L, Schöckel L, *et al* (2017) Mitochondrial ccomplex I inhibition triggers a mitophagy-dependent ROS increase leading to necroptosis and ferroptosis in melanoma cells. <https://doi.org/10.1038/cddis.2017.133>
- Betarbet R, Sherer TB, Greenamyre JT (2002) Animal models of Parkinson's disease. <https://doi.org/10.1002/bies.10067>
- Callizot N, Combes M, Henriques A, Poindron P (2019) Necrosis, apoptosis, necroptosis, three modes of action of dopaminergic neuron neurotoxins. <https://doi.org/10.1371/journal.pone.0215277>
- Cheng G, Zielonka M, Dranka B, Kumar SN, Myers CR, Bennett B, Garces AM, Dias Duarte Machado LG, Thiebaut D, Ouari O, Hardy M, Zielonka J, Kalyanaraman B (2018) Detection of mitochondria-generated reactive oxygen species in cells using multiple probes and methods: potentials, pitfalls, and the future. <https://doi.org/10.1074/jbc.RA118>
- Choi WS, Kruse SE, Palmiter RD, Xia Z (2008) Mitochondrial ccomplex I inhibition is not required for dopaminergic neuron death induced by rotenone, MPP<sup>+</sup>, or paraquat. <https://doi.org/10.1073/pnas.0807581105>
- Dikalov SI, Harrison DG (2014) Methods for detection of mitochondrial and cellular reactive oxygen species. <https://doi.org/10.1089/ars.2012.4886>
- Draper HH, Squires EJ, Mahmoodi H, Wu J, Agarwal S, Hadley M (1993) A comparative evaluation of thiobarbituric acid methods for the determination of malondialdehyde in biological materials. [https://doi.org/10.1016/0891-5849\(93\)90035-s](https://doi.org/10.1016/0891-5849(93)90035-s)
- Duty S, Jenner P (2011) Animal models of Parkinson's disease: a source of novel treatments and clues to the cause of the disease. <https://doi.org/10.1111/j.1476-5381.2011.01426.x>
- Gan B (2021) Mitochondrial regulation of ferroptosis. <https://doi.org/10.1083/jcb.202105043>
- Ganguly G, Chakrabarti S, Chatterjee U, Saso L (2017) Proteinopathy, oxidative stress and mitochondrial dysfunction: cross talk in Alzheimer's disease and Parkinson's disease. <https://doi.org/10.2147/dddt.s130514>
- Ganguly U, Banerjee A, Chakrabarti SS, Kaur U, Sen O, Cappai R, Chakrabarti S (2020) Interaction of  $\alpha$ -synuclein and Parkin in iron toxicity on SH-SY5Y cells: implications in the pathogenesis of Parkinson's disease. <https://doi.org/10.1042/bcj20190676>
- Gao M, Yi J, Zhu J, Minikes AM, Monian P, Thompson CB, Jiang X (2019) Role of mitochondria in ferroptosis. <https://doi.org/10.1016/j.molcel.2018.10.042>
- Gomes A, Fernandes E, Lima JL (2005) Fluorescence probes used for detection of reactive oxygen species. <https://doi.org/10.1016/j.jbbm.2005.10.003>
- Hong Y, Nie H, Wu D, Wei X, Ding X, Ying Y (2014) NAD(+) treatment prevents rotenone-induced apoptosis and necrosis of differentiated PC12 cells. <https://doi.org/10.1016/j.neulet.2013.11.039>
- Jana S, Sinha M, Chanda D, Roy T, Banerjee K, Munshi S, Patro BS, Chakrabarti S (2011) Mitochondrial dysfunction mediated by quinone oxidation products of dopamine: Implications in dopamine cytotoxicity and pathogenesis of Parkinson's disease. <https://doi.org/10.1016/j.bbadis.2011.02.013>

- Jiang X, Stockwell BR, Conrad M (2021) Ferroptosis: mechanisms, biology and role in disease. <https://doi.org/10.1038/s41580-020-00324-8>
- Kabiraj P, Valenzuela CA, Marin JE, Ramirez DA, Mendez L, Hwang MS, Varela-Ramirez A, Fenelon K, Narayan M, Skouta R (2015) The neuroprotective role of ferrostatin-1 under rotenone-induced oxidative stress in dopaminergic neuroblastoma cells. <https://doi.org/10.1007/s10930-015-9629-7>
- Kalyanaraman B, Darley-Usmar V, Davies KJ, Dennerly PA, Forman HJ, Grisham MB, Mann GE, Moore K, Roberts LJ 2nd, Ischiropoulos H (2012) Measuring reactive oxygen and nitrogen species with fluorescent probes: challenges and limitations. <https://doi.org/10.1016/j.freeradbiomed.2011.09.030>
- Ke M, Chong CM, Zhu Q, Zhang K, Cai CZ, Lu JH, Qin D, Su H (2021) Comprehensive perspectives on experimental models for Parkinson's disease. <https://doi.org/10.14336/ad.2020.0331>
- Kinnally KW, Peixoto PM, Ryu SY, Dejean LM (2011) Is mPTP the gatekeeper for necrosis, apoptosis, or both? <https://doi.org/10.1016/j.bbamcr.2010.09.013>
- Kweon GR, Marks JD, Krencik R, Leung EH, Schumacker PT, Hyland K, Kang UJ (2004) Distinct mechanisms of neurodegeneration induced by chronic complex I inhibition in dopaminergic and non-dopaminergic cells. <https://doi.org/10.1074/jbc.M407336200>
- Li J, Cao F, Yin HL, Huang ZJ, Lin ZT, Mao N, Sun B, Wang G (2020) Ferroptosis: past, present, and future. <https://doi.org/10.1038/s41419-020-2298-2>
- Li N, Ragheb K, Lawler G, Sturgis J, Rajwa B, et al (2003) Mitochondrial complex I inhibitor rotenone induces apoptosis through enhancing mitochondrial reactive oxygen species production. <https://doi.org/10.1074/jbc.M210432200>
- Look MP, Rockstroh JK, Rao GS, Kreuzer KA, Barton S, Lemoch H, Sudhop T, Hoch J, Stockinger K, Spengler U, Sauerbruch T (1997) Serum selenium, plasma glutathione (GSH) and erythrocyte glutathione peroxidase (GSH-Px)-levels in asymptomatic versus symptomatic human immunodeficiency virus-1 (HIV-1)-infection. <https://doi.org/10.1038/sj.ejcn.1600401>
- Moon Y, Lee KH, Park JH, Geum D, Kim K (2005) Mitochondrial membrane depolarization and the selective death of dopaminergic neurons by rotenone: protective effect of coenzyme Q10. <https://doi.org/10.1111/j.1471-4159.2005.03112.x>
- Newhouse K, Hsuan SL, Chang SH, Cai B, Wang Y, Xia Z (2004) Rotenone-induced apoptosis is mediated by p38 and JNK MAP kinases in human dopaminergic SH-SY5Y cells. <https://doi.org/10.1093/toxsci/kfh089>
- Radad K, Rausch WD, Gille G (2006) Rotenone induces cell death in primary dopaminergic culture by increasing ROS production and inhibiting mitochondrial respiration. <https://doi.org/10.1016/j.neuint.2006.02.003>
- Rahman I, Kode A, Biswas SK (2006) Assay for quantitative determination of glutathione and glutathione disulfide levels using enzymatic recycling method. <https://doi.org/10.1038/nprot.2006.378>
- Redza-Dutordoir M, Averill-Bates DA (2016) Activation of apoptosis signalling pathways by reactive oxygen species. <https://doi.org/10.1016/j.bbamcr.2016.09.012>
- Richardson JR, Caudle WM, Guillot TS, Watson JL, Nakamaru-Ogiso E, et al (2007) Obligatory role for complex I inhibition in the dopaminergic neurotoxicity of 1-methyl-4-phenyl-1,2,3,6-tetrahydropyridine (MPTP). <https://doi.org/10.1093/toxsci/kfl133>
- Schapira AHV, Cooper JM, Dexter D, Clark JB, Jenner P, Marsden CD (1990) Mitochondrial complex I deficiency in Parkinson's disease. <https://doi.org/10.1111/j.1471-4159.1990.tb02325.x>
- Sherer TB, Betarbet R, Testa CM, Seo BB, Richardson JR, Kim JH, Miller GW, Yagi T, Matsuno-Yagi A, Greenamyre JT (2003) Mechanism of toxicity in rotenone models of Parkinson's disease. <https://doi.org/10.1523/JNEUROSCI.23-34-10756.2003>
- Singh S, Ganguly U, Pal S, Chandan G, Thakur R, Saini RV, Chakrabarti SS, Agrawal BK, Chakrabarti S (2022) Protective effects of cyclosporine A on neurodegeneration and motor impairment in rotenone-induced experimental models of Parkinson's disease. <https://doi.org/10.1016/j.ejphar.2022>

- Smith PK, Krohn RI, Hermanson GT, Mallia AK, Gartner FH, Provenzano MD, Fujimoto EK, Goeke NM, Olson BJ, Klenk DC (1985) Measurement of protein using bicinchoninic acid. [https://doi.org/10.1016/0003-2697\(85\)90442-7](https://doi.org/10.1016/0003-2697(85)90442-7)
- Stockwell BR, Angeli JPF, Bayir H, Bush AI, Conrad M (2017) Ferroptosis: A regulated cell death nexus linking metabolism, redox biology, and disease. <https://doi.org/10.1016/j.cell.2017.09.021>
- Toulorge D, Schapira AHV, Hajj R (2016) Molecular changes in the postmortem Parkinsonian brain. <https://doi.org/10.1111/jnc.13696>
- Urrutia PJ, Aguirre P, Tapia V, Carrasco CM, Mena NP, Núñez MT (2017) Cell death induced by mitochondrial complex I inhibition is mediated by Iron Regulatory Protein 1. <https://doi.org/10.1016/j.bbadis.2017.05.015>
- Wang H, Liu C, Zhao Y, Gao G (2020) Mitochondria regulation in ferroptosis. <https://doi.org/10.1016/j.ejcb.2019.151058>
- Wu C, Zhao W, Yu J, Li S, Lin L, Chen X (2018) Induction of ferroptosis and mitochondrial dysfunction by oxidative stress in PC12 cells. <https://doi.org/10.1038/s41598-017-18935-1>
- Xicoy H, Wieringa B, Martens GJM (2017) The SH-SY5Y cell line in Parkinson's disease research: a systematic review. <https://doi.org/10.1186/s13024-017-0149-0>
- Xie Y, Hou W, Song X, Yu Y, Huang J, Sun X, Kang R, Tang D (2016) Ferroptosis: process and function. <https://doi.org/10.1038/cdd.2015.158>
- Xiong N, Xiong J, Jia M, Liu L, Zhang X, Chen Z, Huang J, Zhang Z, Hou L, Luo Z, Ghoorah D, Lin Z, Wang T (2013) The role of autophagy in Parkinson's disease: rotenone-based modeling. <https://doi.org/10.1186/1744-9081-9-13>
- Yao X, Li W, Fang D, Xiao C, Wu X, Li M, Luo Z (2021) Emerging roles of energy metabolism in ferroptosis regulation of tumor cells. <https://doi.org/10.1002/advs.20210099>
- Zilka O, Shah R, Li B, Friedmann Angeli JP, Griesser M, Conrad M, Pratt DA (2017) On the mechanism of cytoprotection by ferrostatin-1 and liproxstatin-1 and the role of lipid peroxidation in ferroptotic cell death. <https://doi.org/10.1021/acscentsci.7b00028>

**Copyright:** © 2022 The authors. This is an Open Access preprint (not peer-reviewed) distributed under the terms of the Creative Commons Attribution License, which permits unrestricted use, distribution, and reproduction in any medium, provided the original authors and source are credited. © remains with the authors, who have granted MitoFit Preprints an Open Access publication license in perpetuity.

